



UNIVERSITY OF LEEDS

This is a repository copy of *Computable theoretical error bounds for Nyström methods for 1-D Fredholm integral equations of the second kind*.

White Rose Research Online URL for this paper:
<http://eprints.whiterose.ac.uk/90237/>

Version: Accepted Version

Proceedings Paper:

Fairbairn, AI and Kelmanson, MA (2015) Computable theoretical error bounds for Nyström methods for 1-D Fredholm integral equations of the second kind. In: Harris, P, (ed.) Proceedings of the 10th UK Conference on Boundary Integral Methods. 10th UK Conference on Boundary Integral Methods, 13-14 Jul 2015, University of Brighton. University of Brighton . ISBN 1910172057

Reuse

Unless indicated otherwise, fulltext items are protected by copyright with all rights reserved. The copyright exception in section 29 of the Copyright, Designs and Patents Act 1988 allows the making of a single copy solely for the purpose of non-commercial research or private study within the limits of fair dealing. The publisher or other rights-holder may allow further reproduction and re-use of this version - refer to the White Rose Research Online record for this item. Where records identify the publisher as the copyright holder, users can verify any specific terms of use on the publisher's website.

Takedown

If you consider content in White Rose Research Online to be in breach of UK law, please notify us by emailing eprints@whiterose.ac.uk including the URL of the record and the reason for the withdrawal request.



eprints@whiterose.ac.uk
<https://eprints.whiterose.ac.uk/>

0 Computable theoretical error bounds for Nyström methods for 1-D Fredholm integral equations of the second kind

Abigail I Fairbairn and Mark A Kelmanson[†]

Department of Applied Mathematics, University of Leeds, Leeds LS2 9JT
mm09af@leeds.ac.uk and mark@maths.leeds.ac.uk ([†]corresponding author)

Abstract

New expressions for computable error bounds are derived for Nyström-method approximate solutions of one-dimensional second-kind Fredholm integral equations. The bounds are computed using *only the numerical solution*, and so require no *a priori* knowledge of the exact solution. The analysis is implemented on test problems with both well-behaved and “Runge-phenomenon” solutions, and the computed predictions are shown to be in impressive quantitative agreement with the true errors obtained from known exact solutions of the test problems. For independent computational validation, both Lagrange and barycentric interpolation are employed on grids with both regularly spaced nodes and those located at the roots or extrema of orthogonal polynomials. For independent theoretical validation, asymptotic estimates are derived for the convergence rates of the observed computational errors.

0.1 Introduction

Presented herein is the theory for, and implementation of, a new method for computing explicit *a priori* bounds for the error in the numerical approximation of solutions of linear Fredholm integral equations of the second kind (FIE2s). Since the theory is based on Nyström-type quadrature methods that utilise nodes based on both Chebyshev and Legendre polynomials, it is assumed that the FIE2s have been *a priori* scaled onto the universal interval $[-1, 1]$, so that the FIE2 under consideration is of the canonical form

$$u(x) - \lambda \int_{-1}^1 K(x, y) u(y) dy = f(x), \quad x \in [-1, 1], \quad (0.1)$$

in which $u(x)$ is the required solution, $K(x, y)$ is the kernel, $f(x)$ is the source function and λ is a real or complex constant. It is assumed that u , K and f are bounded and infinitely differentiable for $x, y \in [-1, 1]$, and that λ is not a characteristic value of (0.1), which therefore has the unique solution $u(x)$.

The approximate numerical solution of (0.1) is considered in a substantial literature, of which [1, 2, 3, 4] are perhaps the best known fundamental treatises covering the theory and implementation of a host of methods (e.g. interpolation, projection, collocation and quadrature) that attest to the widespread and continuing interest in (0.1). Despite the demonstrable interest in the development of such methods, implementation of quantifiable analyses for estimating computable *a priori* error bounds for them continues to be relatively scarce in the literature; indeed, it is acknowledged [2, p.158] that “*these bounds will be difficult to evaluate in applications*”. In particular, it is explicitly noted [5] that, in the “*actual numerical computation [of error bounds]*”, there are “*only some scattered results that apply this approach.*” For example, when (0.1) is of degenerate-kernel form, computable error bounds can readily be computed [4, p.32] and, for the general form of (0.1), error estimates based on Gauss-Jacobi polynomials can be found [6] within the context of Nyström-based methods.

Thus motivated, the error analysis developed herein is founded on an operator theory that underpins both convergence and stability analyses of the Nyström method within a general abstract framework. Specifically, the present work demonstrates that accurate error estimates can be obtained by building upon and extending two fundamental interconnected theorems, [3, Thm. 4.7.11] and [4, Thm. 4.1.1], in such a

way that the approximate solution of (0.1) can be used to yield accurate *a priori* error predictions in the absence of an exact solution. The new prediction differs markedly from the *a posteriori* error estimate [7, (14,15)] inherent in “forced-oscillation” interpolation [8, (4.7.39)] which, as demonstrated in §0.4, is orders of magnitude larger than the Nyström error. Finally, it is noted that the present approach aligns with the recent interest in, and development of, fast and spectrally accurate algorithms [9] for computing the nodes and weights of Gaussian quadratures utilising in excess of 100 nodes.

The remainder of this paper is structured as follows. In §0.2.1 and §0.2.2 are presented overviews of, respectively, the “classic” and “interpolated” Nyström method (CNM and INM), in the latter of which both Lagrange and barycentric interpolation are used to project between Nyström and, e.g., optimal differentiation nodes. In §0.3 are presented error analyses for both the CNM and INM on meshes that used nodes that are either regularly spaced or at the roots and extrema of orthogonal polynomials. In §0.4 are presented numerical results generated by implementing the new theory, validation of which is convincingly demonstrated by application to test problems for which exact solutions of (0.1) are known. One such solution is infinitely continuously differentiable; interpolation of the other is plagued by the Runge phenomenon on the regular mesh, the consequences of which are analysed explicitly and explained via an asymptotic analysis. The summary in §0.5 includes brief suggestions of how the estimates can be further improved in future work.

0.2 Nyström Method

0.2.1 Classic Version

Following, e.g., [4], (0.1) can be written in symbolic form as

$$u - \lambda \mathcal{K} u = f, \quad (0.2)$$

in which the action of the integral operator \mathcal{K} on u is defined by

$$\mathcal{K} u = (\mathcal{K} u)(x) \equiv \int_{-1}^1 K(x, y) u(y) dy. \quad (0.3)$$

In the Nyström method, the action of the integral operator \mathcal{K} is approximated by an operator \mathcal{K}_N that represents an N -node quadrature rule, thereby yielding the discrete counterpart,

$$\mathcal{K} u \approx \mathcal{K}_N u = (\mathcal{K}_N u)(x) \equiv \sum_{j=1}^N w_{j,N} K(x, y_{j,N}) u(y_{j,N}), \quad (0.4)$$

of (0.3), in which $w_{j,N}$ and $y_{j,N}$ are respectively the weights and abscissae of the rule. Because the weight function in the integral in (0.3) is unity, Gauss-Legendre quadrature (GLQ) is used [10, Table 4.4], which yields the weights $w_{j,N}$ and abscissae $y_{j,N}$ that maximise the order of the quadrature rule. This is tantamount to interpolating $u(x)$ on $[-1, 1]$ by Legendre polynomials, whence the abscissae $y_{j,N}$ are simply the zeros of the Legendre polynomial of the first kind, $P_N(x)$, of degree N ,

$$P_N(y_{j,N}) = 0, \quad j = 1(1)N, \quad (0.5)$$

with the weights $w_{j,N}$ then given by

$$w_{j,N} = \frac{-2}{(N+1) P'_N(y_{j,N}) P_{N+1}(y_{j,N})}, \quad j = 1(1)N. \quad (0.6)$$

Using (0.4), a discrete equation is obtained for the (GLQ-)Nyström approximation, $u_N(x)$, of (0.1), which satisfies

$$u_N(x) - \lambda \sum_{j=1}^N w_{j,N} K(x, y_{j,N}) u_N(y_{j,N}) = f(x), \quad x \in [-1, 1], \quad (0.7)$$

with corresponding symbolic form

$$u_N - \lambda \mathcal{K}_N u_N = f. \quad (0.8)$$

Collocating (0.7) at the N nodes $x = y_{i,N}$, $i = 1(1)N$, yields

$$u_N(y_{i,N}) - \lambda \sum_{j=1}^N w_{j,N} K(y_{i,N}, y_{j,N}) u_N(y_{j,N}) = f(y_{i,N}), \quad i = 1(1)N, \quad (0.9)$$

which is an $N \times N$ linear system for the nodal values $u_N(y_{j,N})$, $j = 1(1)N$ which, in matrix-vector form, is

$$(\mathbf{I} - \lambda \mathbf{K}_N) \mathbf{u}_N = \mathbf{f}_N, \quad (0.10)$$

wherein the elements, for $i, j = 1(1)N$, are given by the explicit formulae

$$\{\mathbf{u}_N\}_i = u_N(y_{i,N}), \quad \{\mathbf{f}_N\}_i = f(y_{i,N}), \quad \{\mathbf{K}_N\}_{i,j} = w_{j,N} K(y_{i,N}, y_{j,N}). \quad (0.11)$$

Inversion of the system (0.10) yields the nodal values $u_N(y_{j,N})$, $j = 1(1)N$ in the Nyström inversion formula

$$u_N(x) = f(x) + \lambda \sum_{j=1}^N w_{j,N} K(x, y_{j,N}) u_N(y_{j,N}), \quad x \in [-1, 1], \quad (0.12)$$

which is used to approximate $u(x)$ for all $x \in [-1, 1]$. Finally, it is noted that, by (0.9), (0.12) and the construction of GLQ, it is the case that $u_N(x) \equiv u(x)$ if the product $K(x, y) u(y)$ in (0.1) is a polynomial in y of degree less than or equal to $2N - 1$.

0.2.2 Interpolated Version

By the discussion immediately after (0.4), the classical Nyström method (CNM) utilises abscissae at the roots of the Legendre polynomials $P_N(x)$ since the weight function (implied) in (0.1) is unity. However, within the context of, for example, integro-differential equations (IDEs), the error in approximating differentiation is optimised when the nodes are at the roots of the Chebyshev polynomials $T_N(x)$ [11]. In this event, interpolation between the Legendre and Chebyshev nodal data is demanded by the need to minimise the total error. In this context, analysis of a new ‘‘interpolated Nyström method’’ (INM) is presented, although implementation of the full solution of IDEs is deferred to a companion paper.

In the quadrature rule on the right-hand side of (0.7), the nodal ordinates $u_N(y_{j,N})$ are Lagrange-interpolated through a set of nodes $\{\tilde{y}_{k,N}\}_{k=1}^N \subseteq [-1, 1]$ that are distinct from the Legendre nodes $\{y_{j,N}\}_{j=1}^N$ defined by (0.5). Corresponding to (0.7), the new ‘‘interpolated Nyström’’ approximation \tilde{u}_N therefore satisfies, for $x \in [-1, 1]$,

$$\tilde{u}_N(x) - \lambda \sum_{j=1}^N w_{j,N} K(x, y_{j,N}) \sum_{k=1}^N L_{k,N}(y_{j,N}) \tilde{u}_N(\tilde{y}_{k,N}) = f(x),$$

whose symbolic form is

$$\tilde{u}_N - \lambda \mathcal{K}_N \mathcal{L}_N \tilde{u}_N = f, \quad (0.13)$$

in which the action of the operator \mathcal{L}_N is defined by

$$\mathcal{L}_N \tilde{u}_N = (\mathcal{L}_N \tilde{u}_N)(x) \equiv \sum_{k=1}^N L_{k,N}(x) \tilde{u}_N(\tilde{y}_{k,N}), \quad x \in [-1, 1], \quad (0.14)$$

wherein the Lagrange basis functions are given by

$$L_{k,N}(x) = \prod_{\substack{\ell=1 \\ \ell \neq k}}^N \frac{x - \tilde{y}_{\ell,N}}{\tilde{y}_{k,N} - \tilde{y}_{\ell,N}}, \quad k = 1(1)N. \quad (0.15)$$

Collocating (0.13) at the N (new) nodes $x = \tilde{y}_{i,N}$, $i = 1(1)N$ and interchanging the subscripts j and k yields an $N \times N$ linear system for the nodal values $\tilde{u}_N(\tilde{y}_{j,N})$, $j = 1(1)N$ which, in matrix-vector form, is

$$(\mathbf{I} - \lambda \tilde{\mathbf{K}}_N) \tilde{\mathbf{u}}_N = \mathbf{f}_N, \quad (0.16)$$

wherein the elements, for $i, j = 1(1)N$, are given by the explicit formulae

$$\begin{aligned} \{\tilde{\mathbf{u}}_N\}_i &= \tilde{u}_N(\tilde{y}_{i,N}), \quad \{\mathbf{f}_N\}_i = f(\tilde{y}_{i,N}), \\ \{\tilde{\mathbf{K}}_N\}_{i,j} &= \sum_{k=1}^N w_{k,N} K(\tilde{y}_{i,N}, y_{k,N}) L_{j,N}(y_{k,N}). \end{aligned} \quad (0.17)$$

Inversion of (0.16) yields the nodal values $\tilde{u}_N(\tilde{y}_{j,N})$, $j = 1(1)N$ for computing the approximate solution $\tilde{u}_N(x)$, for $x \in [-1, 1]$, of (0.1) via the inversion formula

$$\tilde{u}_N(x) = f(x) + \lambda \sum_{k=1}^N w_{k,N} K(x, y_{k,N}) \sum_{j=1}^N L_{j,N}(y_{k,N}) \tilde{u}_N(\tilde{y}_{j,N}). \quad (0.18)$$

Note that the price paid for utilising independent integration and interpolation nodes is, by comparing (0.11) with (0.17), the order $O(N)$ summation required within each element of the amended system matrix $\tilde{\mathbf{K}}_N$.

0.3 Error Analysis

The CNM is first analysed. Subtracting (0.8) from (0.2) yields

$$u - u_N = \lambda (\mathcal{K} u - \mathcal{K}_N u_N) = \lambda \mathcal{K} (u - u_N) + \lambda (\mathcal{K} - \mathcal{K}_N) u_N,$$

hence the error can be expressed in terms of (only) the approximate solution u_N as

$$u - u_N = \lambda (\mathcal{I} - \lambda \mathcal{K})^{-1} (\mathcal{K} - \mathcal{K}_N) u_N, \quad (0.19)$$

in which the existence and boundedness of $(\mathcal{I} - \lambda \mathcal{K})^{-1}$ is guaranteed [2, Thm. 3.4] by u being the unique solution of (0.2), equivalently $(\mathcal{I} - \lambda \mathcal{K}) u = f$, and in which (0.8) gives $\lambda (\mathcal{K} - \mathcal{K}_N) u_N = \lambda \mathcal{K} u_N - u_N + f$. Thus an error bound for the CNM is

$$\|u - u_N\| \leq \|(\mathcal{I} - \lambda \mathcal{K})^{-1}\| \|u_N - \lambda \mathcal{K} u_N - f\|, \quad (0.20)$$

which, to the authors' knowledge, is a novel way of expressing the error that both avoids having to compute $\mathcal{K}_N u_N$ and admits the "inverted" interpretation of the degree to which the exact operator \mathcal{K} fails to approximate the Nyström operator \mathcal{K}_N in the equation (0.8) for u_N . In (0.20), and subsequently, the infinity

norm $\|\cdot\|$ defined on $[-1, 1]$ is used, and a bound for the first term on the right-hand side can be obtained as (cf. [3, (4.7.17b)])

$$\|(\mathcal{I} - \lambda \mathcal{K})^{-1}\| \leq \frac{1 + |\lambda| \|\mathcal{I} - \lambda \mathcal{K}_N\| \|\mathcal{K}\|}{1 - \lambda^2 \|(\mathcal{I} - \lambda \mathcal{K}_N)^{-1}\| \|(\mathcal{K} - \mathcal{K}_N) \mathcal{K}\|}. \quad (0.21)$$

Being derived via the geometric series theorem [1, Thm. 1.1], both numerator and denominator on the right-hand side of (0.21) are by construction positive (cf. [4, (4.1.22)]): additionally, $(\mathcal{I} - \lambda \mathcal{K}_N)^{-1}$ exists and is bounded via the existence and uniqueness of the solution u of (0.2) [4, Thm. 4.1.2].

Though alternative bounds have been presented in the sources cited, they have been neither expressed in the simple form (0.20) nor used for the explicit computation of $\|u - u_N\|$. Pursuing this objective, $\nu_N > 0$ and $\delta_N > 0$ are used to denote respectively the numerator and denominator of the right-hand side of (0.21). Then, for all N , $\|(\mathcal{I} - \lambda \mathcal{K})^{-1}\| \leq \nu_N / \delta_N$, so the tightest bound on $(\mathcal{I} - \lambda \mathcal{K})^{-1}$ uses the minimum value $\check{\nu}_N$ of ν_N and the maximum value $\hat{\delta}_N$ of δ_N . By (0.21), both $\check{\nu}_N$ and $\hat{\delta}_N$ demand $\|(\mathcal{I} - \lambda \mathcal{K}_N)^{-1}\|$ to be minimised; additionally, $\check{\nu}_N$ and $\hat{\delta}_N$ respectively demand $\|\mathcal{K}\|$ and $\|(\mathcal{K} - \mathcal{K}_N) \mathcal{K}\|$ to be minimised. Applying standard norm properties to the inverse of (0.8) yields

$$\|(\mathcal{I} - \lambda \mathcal{K}_N)^{-1}\| \geq \frac{\|u_N\|}{\|f\|}, \quad (0.22)$$

in which equality minimises $\|(\mathcal{I} - \lambda \mathcal{K}_N)^{-1}\|$ as the computable right-hand side. For sufficiently large N , $u_N \approx u$ by construction, whence norm properties yield

$$\|(\mathcal{K} - \mathcal{K}_N) \mathcal{K}\| \equiv \sup_u \frac{\|(\mathcal{K} - \mathcal{K}_N) \mathcal{K} u\|}{\|u\|} \geq \frac{\|(\mathcal{K} - \mathcal{K}_N) \mathcal{K} u\|}{\|u\|} \approx \frac{\|(\mathcal{K} - \mathcal{K}_N) \mathcal{K} u_N\|}{\|u_N\|}, \quad (0.23)$$

of which the last term approximately minimises $\|(\mathcal{K} - \mathcal{K}_N) \mathcal{K}\|$ as a computable quantity, and within which $\mathcal{K} u_N$ can be re-used to minimise $\|\mathcal{K}\|$ in (0.21) without further expense as $\|\mathcal{K} u_N\| / \|u_N\|$; *a posteriori* consideration of the results in §0.4 vindicates both this and the approximation (0.23). Assembling all results, the new prediction of the error bound for the CNM is

$$\|u - u_N\| \leq \frac{\|f\| + |\lambda| \|\mathcal{K} u_N\|}{\|f\| - \lambda^2 \|(\mathcal{K} - \mathcal{K}_N) \mathcal{K} u_N\|} \|u_N - \lambda \mathcal{K} u_N - f\|, \quad (0.24)$$

in which the right-hand side is explicitly computable in terms of only the approximate solution $u_N = f + \lambda \mathcal{K}_N u_N$ determined by (0.8).

Turning to the INM, subtraction of (0.13) from (0.8) yields

$$u - \tilde{u}_N = \lambda(\mathcal{K} u - \mathcal{K}_N \mathcal{L}_N \tilde{u}_N),$$

in which the action of \mathcal{L}_N is defined by (0.14). Proceeding along identical lines to those used in deriving (0.19) and (0.20) now yields the INM error,

$$u - \tilde{u}_N = \lambda(\mathcal{I} - \lambda \mathcal{K})^{-1}(\mathcal{K} - \mathcal{K}_N \mathcal{L}_N) \tilde{u}_N, \quad (0.25)$$

with bound

$$\|u - \tilde{u}_N\| \leq \|(\mathcal{I} - \lambda \mathcal{K})^{-1}\| \|\tilde{u}_N - \lambda \mathcal{K} \tilde{u}_N - f\|, \quad (0.26)$$

which both avoids the need to compute $\mathcal{K}_N \mathcal{L}_N \tilde{u}_N$ and again admits the “inverted” interpretation of the degree to which the exact operator \mathcal{K} fails to approximate the “interpolated Nyström” operator $\mathcal{K}_N \mathcal{L}_N$ in the equation (0.13) for \tilde{u}_N , and in which (0.21) must be amended to

$$\|(\mathcal{I} - \lambda \mathcal{K})^{-1}\| \leq \frac{1 + |\lambda| \|(\mathcal{I} - \lambda \mathcal{K}_N \mathcal{L}_N)^{-1}\| \|\mathcal{K}\|}{1 - \lambda^2 \|(\mathcal{I} - \lambda \mathcal{K}_N \mathcal{L}_N)^{-1}\| \|(\mathcal{K} - \mathcal{K}_N \mathcal{L}_N) \mathcal{K}\|}. \quad (0.27)$$

Repeating the minimum-numerator, maximum-denominator argument used in deriving (0.24) now yields

$$\|u - \tilde{u}_N\| \leq \frac{\|f\| + |\lambda| \|\mathcal{K} \tilde{u}_N\|}{\|f\| - \lambda^2 \|(\mathcal{K} - \mathcal{K}_N \mathcal{L}_N) \mathcal{K} \tilde{u}_N\|} \|\tilde{u}_N - \lambda \mathcal{K} \tilde{u}_N - f\|, \quad (0.28)$$

in which the right-hand side is explicitly computable in terms of only the approximate solution $\tilde{u}_N = f + \lambda \mathcal{K}_N \mathcal{L}_N \tilde{u}_N$ determined by (0.13).

0.4 Implementation, Results and Discussion

The theory of §0.3 is now implemented and validated using two examples of (0.1) for which exact solutions are known. The first, “problem 1”, is

$$\begin{aligned} u(x) &= \frac{1}{10} \int_{-1}^1 (3x+2)(y+1)u(y) dy \\ &= \cos x - \frac{1}{5} \sin(3x+2) - \frac{11}{5}x + \frac{13}{15}, \quad x \in [-1, 1], \end{aligned} \quad (0.29)$$

whose exact solution $u(x) = \cos x - 2x + 1$ is bounded and infinitely continuously differentiable on $x \in [-1, 1]$. The second, “problem 2”, is

$$\begin{aligned} u(x) &= \frac{1}{10} \int_{-1}^1 (3x+2 + (2x-1)(25y^2+1))u(y) dy \\ &= \frac{1}{25x^2+1} + \frac{1}{25}(5-10x - (3x+2)\tan^{-1}5), \quad x \in [-1, 1], \end{aligned} \quad (0.30)$$

whose exact solution $u(x) = 1/(25x^2+1)$ is also bounded and infinitely differentiable on $x \in [-1, 1]$ but which, when interpolated on a regular grid, has an exponentially divergent interpolation error as N increases [11]. Problems 1 and 2 are each solved using both the CNM and an INM that uses three different interpolation node sets located at regular intervals, Chebyshev zeros and Chebyshev extrema. For the sake of compactness and consistency in presenting subsequent results, note that the CNM can be considered to be the INM using interpolation nodes located at the Legendre zeros, in which case $\mathcal{L}_N \equiv \mathcal{I}$.

Since it is well known [12, 13, 14] that barycentric interpolation is more stable and computationally efficient than its Lagrange counterpart (0.14), the alternative barycentric interpolation formula

$$(\mathcal{L}_N \tilde{u}_N)(x) \equiv \sum_{j=1}^N \frac{\tilde{\omega}_{j,N} \tilde{u}_N(\tilde{y}_{j,N})}{x - \tilde{y}_{j,N}} \bigg/ \sum_{j=1}^N \frac{\tilde{\omega}_{j,N}}{x - \tilde{y}_{j,N}}, \quad x \in [-1, 1] \quad (0.31)$$

was used to replace (0.14) in the above to check both accuracy and stability, particularly for larger N ; predicted errors, by construction, remain unaltered. The barycentric weights $\tilde{\omega}_{j,N} = 1/\tilde{\Psi}'_N(\tilde{y}_{j,N})$ in (0.31) were evaluated explicitly [13] for nodes that are regularly spaced, at Chebyshev extrema and at Chebyshev roots. In all cases, it transpired that results computed using either (0.14) or (0.31) were indistinguishable from each other on the scale presented; however, numerical experiments revealed (0.31) to be $\approx O(N)$ times faster than (0.14).

In solving both problems 1 and 2 on the four described node sets, the INM solution \tilde{u}_N was computed in two ways. Having first solved (0.16) for the nodal values $\tilde{u}_N(\tilde{y}_{j,N})$, $j = 1(1)N$, the solution $\tilde{u}_N(x)$ for $x \in [-1, 1]$ was computed using either Lagrange interpolation $\tilde{u}_N(x) = \mathcal{L}_N \tilde{u}_N$ (cf. (0.14), “method 1”) or Nyström inversion $\tilde{u}_N(x) = f + \lambda \mathcal{K}_N \mathcal{L}_N \tilde{u}_N$ (cf. (0.18), “method 2”).

The effect upon the error of the type of interpolation is first considered. In figures 0.1(a) and 0.1(b) are respectively presented semilog plots of the true (computational) error $e_N \equiv \|u - \tilde{u}_N\|$ for problems 1 (0.29) and 2 (0.30), for each of which \tilde{u}_N is evaluated using both interpolations (0.14) (method 1) and

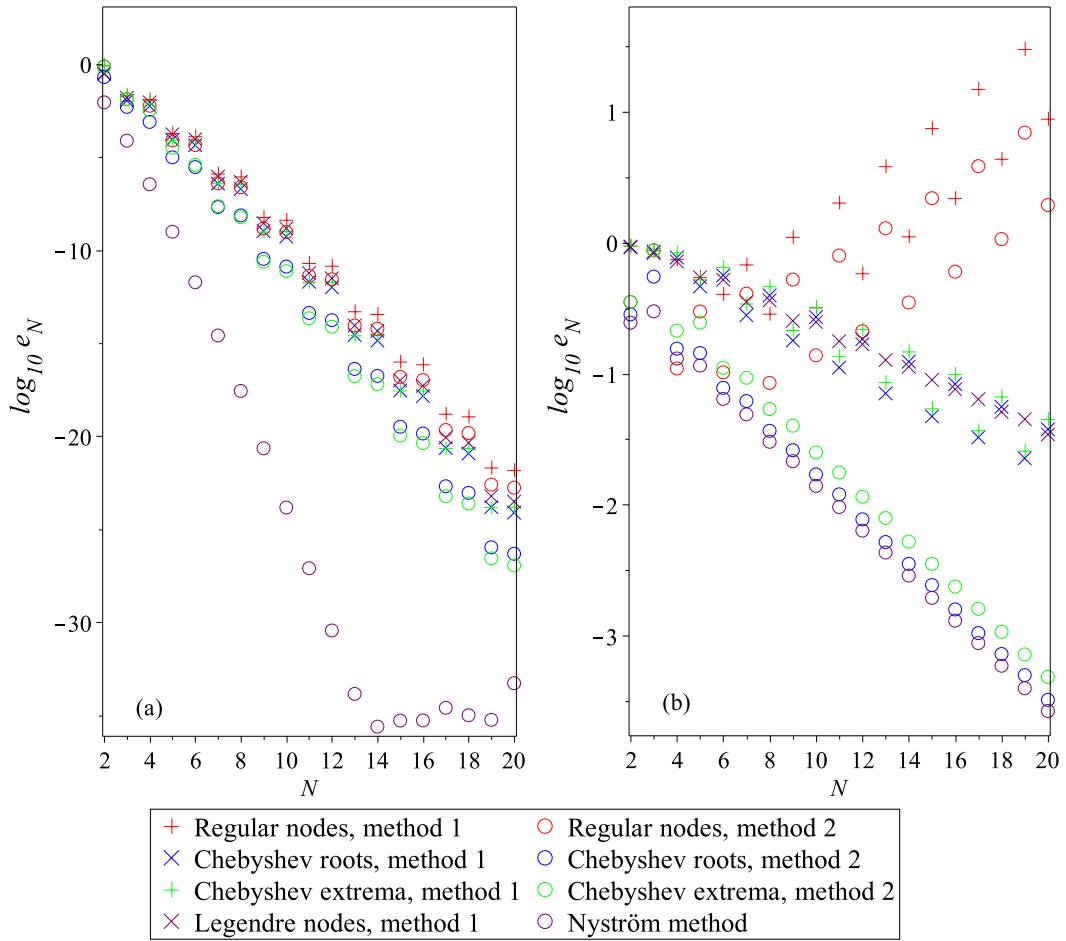


Figure 0.1: *Semilog plots of the true (computational) INM error $e_N \equiv \|u - \tilde{u}_N\|$ for (a) problem 1 (0.29), and (b) problem 2 (0.30), in both of which \tilde{u}_N is computed using interpolations (0.14) (method 1) and (0.18) (method 2). In (a), note the optimal performance of the CNM (the INM on Legendre nodes), the uniform superiority of method 2 over method 1, and the spectral convergence of both methods. In (b), note the expected manifestation (divergence) of the Runge phenomenon on the regularly spaced nodes and, by comparing the vertical scale with that in (a), the uniform erosion of error convergence rate on the orthogonal-polynomial nodes.*

(0.18) (method 2). For problem 1, immediately evident in figure (0.1)(a) is the superior performance of INM method 2 interpolated on the Legendre nodes—i.e. the CNM—in which the error roundoff plateau (for the 36-digit arithmetic used here) is rapidly achieved. Moreover, the vertical scale reveals that the INM error (for both methods 1 and 2) on all other node sets still converges to zero spectrally with N , in keeping with the behaviour demanded of the INM in its intended application to IDEs.

The divergence of errors with N shown in figures 0.1(b) demonstrates the expected failure of both INM methods 1 and 2 when the solution $u(x) = 1/(25x^2 + 1)$ of problem 2 is interpolated at regularly spaced nodes: this is the manifestation of the well-known Runge phenomenon [11] associated with the interpolation of $u(x)$ on $[-1, 1]$ which, whilst not fatal to the INM on the orthogonal-polynomial nodal distributions, greatly reduces the efficacy of the method thereon, as evidenced by comparing vertical scales in figures (0.1)(a) and (b).

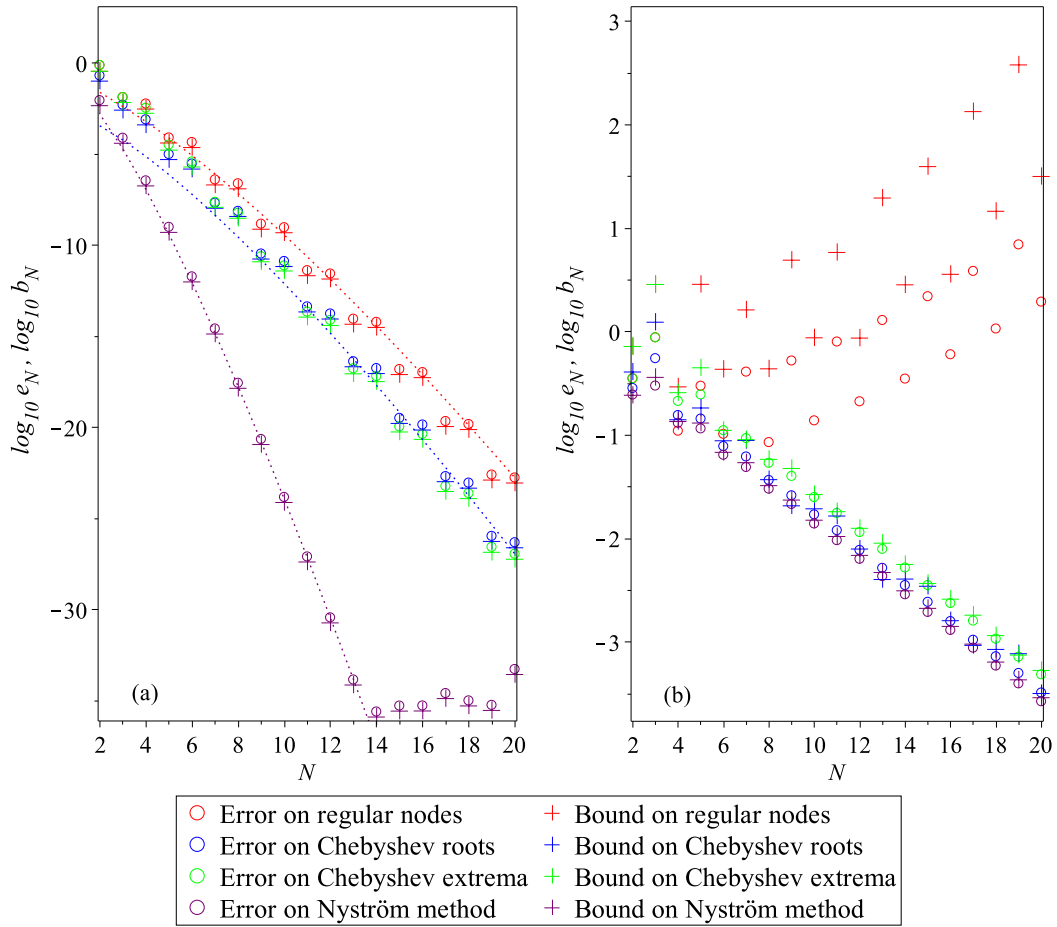


Figure 0.2: Semilog plots of the true (computational) INM error $e_N \equiv \|u - \tilde{u}_N\|$ and bound b_N predicted by (0.28) for (a) problem 1 (0.29), and (b) problem 2 (0.30), in which \tilde{u}_N is computed using interpolation (0.18) (method 2). In (a), note the demonstrable impressive accuracy of the predictions irrespective of the interpolation nodes. In (b), note that, on the regular nodes, the Runge phenomenon that causes the true error e_N to diverge exponentially also does so for the predicted bound b_N . The dotted lines in (a) indicate the theoretical (asymptotic) convergence rates (0.32) that explain the marked disparity in the CNM and INM errors for problem 1.

In figure 0.2 are presented both the true errors e_N and the newly predicted error bounds b_N for problems 1 and 2, as solved using INM method 2 on different interpolation nodes. In figure 0.2(a), which has the same axis scaling as figure 0.1(a), note that both the CNM and INM errors for problem 1 are predicted extremely accurately by the computable bounds (0.24) and (0.28) respectively. Note also that the CNM error is orders of magnitude smaller than the INM error in this case. This discrepancy is now quantified.

Using well-known formulae for the errors incurred in both Lagrange interpolation [8, (5.3.29)] and GLQ [8, (4.7.26)], it is possible to use the exact solution u and kernel K in (0.1) to derive leading-order explicit asymptotic estimates for the convergence rates (ignoring numerical prefactors) of the error e_N as $N \rightarrow \infty$. If a superscript in parentheses denotes the degree of partial differentiation with respect to y , it can be shown that the bounds necessary for the interpolation and GLQ errors are respectively $\|u^{(N)}\| = O(1)$ and $\|(K u)^{(2,N)}\| = O(N)$. Omitting algebraic details, the INM convergence rates for e_N in problem 1 can

be shown to be

$$\frac{N}{4^N (2N)!}, \quad \frac{1}{2^N N!} \quad \text{and} \quad \frac{1}{N} \left[\frac{2}{N-1} \right]^N \quad (0.32)$$

for Legendre nodes (i.e. the CNM), Chebyshev nodes or extrema, and regularly spaced nodes respectively. Appropriate scalar multiples of the theoretical rates (0.32) are superimposed on the numerical errors e_N and computed bounds b_N in figure 0.2(a). The agreement is excellent, confirming that (0.32) fully explains the large disparity between the CNM and INM accuracies for the “well-behaved” problem 1.

The corresponding results for problem 2 are presented in figure 0.2(b), the bottom half of which contains a vertically compressed version of the true errors plotted in figure 0.1(b), and the top half of which reveals that, as expected, when regularly spaced nodes are employed for INM interpolation, the predicted INM error bounds no longer approximate well the true INM errors. This breakdown is again a manifestation of the Runge phenomenon. However, by contrast with problem 1, the convergence rate of e_N cannot be explicitly predicted because the theoretical bounds $\|u^{(N)}\| \leq N! \alpha^N$ and $\|(K u)^{(2N)}\| \leq (2N)! \alpha^{2N}$ are over-pessimistic to the extent that they portend a divergence of e_N , on even the Legendre and Chebyshev nodes, that is not validated by the numerical results shown in figure 0.2(b). In this case, all that can be predicted is that the convergence rates of both the GLQ and interpolation errors are of the same order, and that the spectral convergence of the CNM degenerates to pure-exponential convergence, as evidenced by the linearity of the convergence rates in the semilog plot figure 0.2(b).

0.5 Summary

A novel error analysis has been developed for the (GLQ) Nyström method, for which errors are well-known to be “*difficult to estimate*” [8, p.282]. The analysis has been demonstrated to yield accurate prediction of errors via unexpectedly simple to state and hitherto-unknown explicit computations that utilise only the computed numerical solution. For FIE2s in which the solution is infinitely continuously and boundedly differentiable, computed error estimates are spectrally accurate and error convergence rates have been predicted *a priori*. When higher derivatives of the solution are unbounded, discrepancies between the CNM and INM errors can be explicitly analysed so that the observed quantitative breakdown of the approach in the presence of the Runge phenomenon can be accurately quantified. Ongoing work is aimed at improving the estimates (0.22) and (0.23) of required norm approximations in order to preclude the situation, observed for the test problems herein, that the predicted bounds are marginally lower than the true errors.

References

- [1] C.T.H. Baker. *The Numerical Treatment of Integral Equations*. Clarendon Press, Oxford, 1977.
- [2] R. Kress. *Linear Integral Equations*. Springer Verlag, Heidelberg, 1989.
- [3] W. Hackbusch. *Integral Equations: Theory and Numerical Treatment*. Birkhäuser Verlag, Berlin, 1995.
- [4] K.E. Atkinson. *The Numerical Solution of Integral Equations of the Second Kind*. Cambridge University Press, New York, 1997.
- [5] P. Linz. Bounds and estimates for condition numbers of integral equations. *SIAM J. Numer. Anal.*, 28(1):227–235, 1991.
- [6] M.A. Kelmanson and M.C. Tenwick. Error reduction in Gauss-Jacobi-Nyström quadrature for Fredholm integral equations of the second kind. *CMES-Comp. Model. Eng.*, 55(2):191–210, 2010.

- [7] L. Brutman. An application of the generalized alternating polynomials to the numerical solution of Fredholm integral equations. *Numer. Alg.*, 5:437–442, 1993.
- [8] K.E. Atkinson. *An Introduction to Numerical Analysis*. Wiley, Singapore, 2nd edition, 1989.
- [9] N. Hale and A. Townsend. Fast and accurate computation of Gauss-Legendre and Gauss-Jacobi quadrature nodes and weights. *SIAM J. Sci. Comput.*, 35(2):A652–A674, 2013.
- [10] A. Ralston and P. Rabinowitz. *A First Course in Numerical Analysis*. Dover Publications, Mineola, New York, 2001.
- [11] J.P. Boyd. Defeating the Runge Phenomenon for equispaced polynomial interpolation via Tikhonov regularization. *Appl. Math. Lett.*, 5(6):57–59, 1992.
- [12] H.E. Salzer. Lagrangian interpolation at the Chebyshev points $x_{n,\nu} \equiv \cos(\nu\pi/n)$, $\nu = 0(1)n$; some unnoted advantages. *Comput. J.*, 15(2):156–159, 1972.
- [13] J.P. Berrut and L.N. Trefethen. Barycentric Lagrange interpolation. *SIAM Rev.*, 46(3):501–517, 2004.
- [14] N.J. Higham. The numerical stability of barycentric Lagrange interpolation. *IMA J. Numer. Anal.*, 24:547–556, 2004.